

# Supplementary information

## Nucleus-Translocated GCLM Promotes Chemoresistance in Colorectal Cancer through a Moonlighting Function

Jin-Fei Lin, Ze-Xian Liu, Dong-Liang Chen, Ren-Ze Huang, Fen Cao, Kai Yu, Ting Li, Hai-Yu Mo, Hui Sheng, Zhi-Bing Liang, Kun Liao, Yi Han, Shan-Shan Li, Zhao-Lei Zeng, Song Gao, Huai-Qiang Ju, Rui-Hua Xu

**Supplementary Figure 1:** GCLM depletion enhances the chemosensitivity of CRC cells to oxaliplatin.

**Supplementary Figure 2:** GCLM translocates to the nucleus up platinum drug treatment.

**Supplementary Figure 3:** Nuclear GCLM interacts with NKRF to orchestrate NF- $\kappa$ B activity and chemoresistance.

**Supplementary Figure 4:** Platinum drugs promote GCLM nuclear localization via GCLM binding to importin  $\alpha$ 5.

**Supplementary Figure 5:** P38 MPAK-mediated phosphorylation of GCLM participates in platinum drug-induced nuclear localization of GCLM.

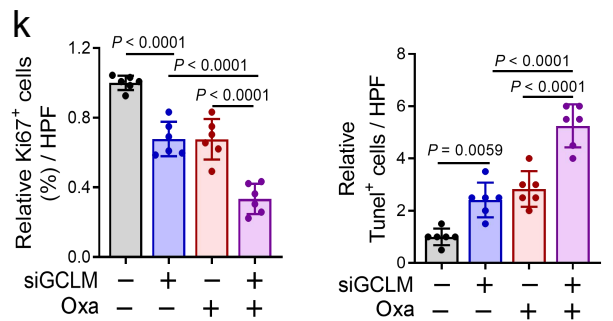
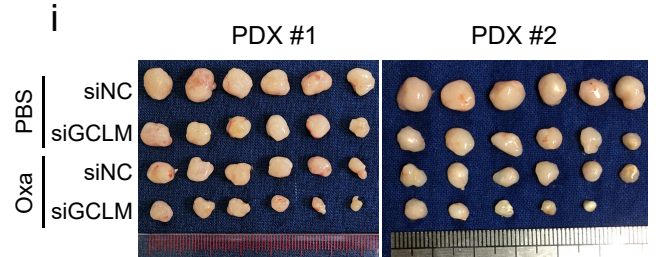
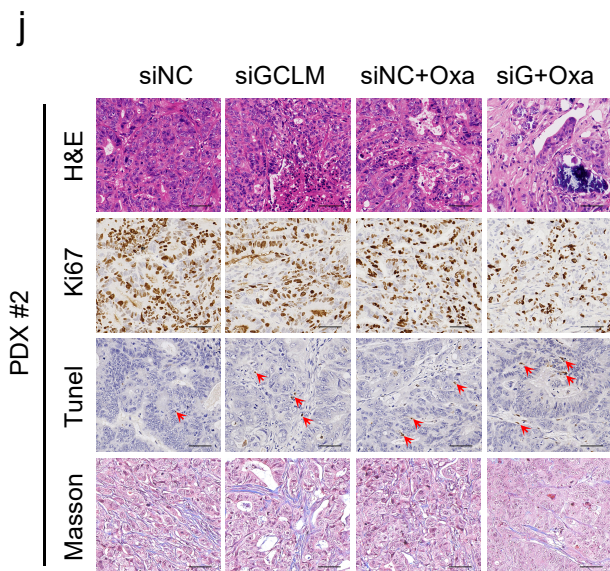
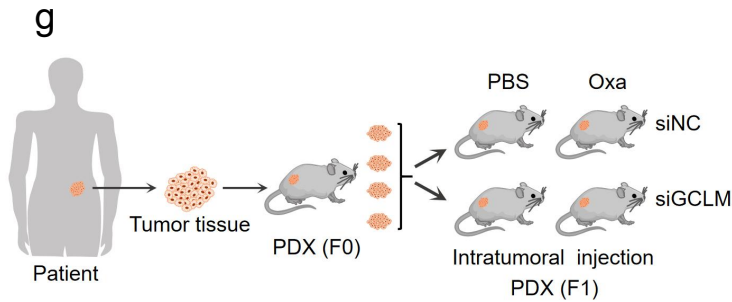
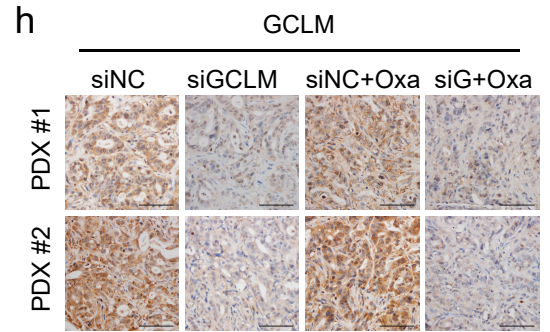
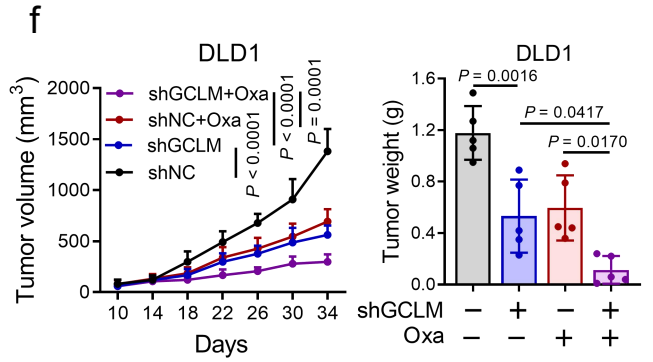
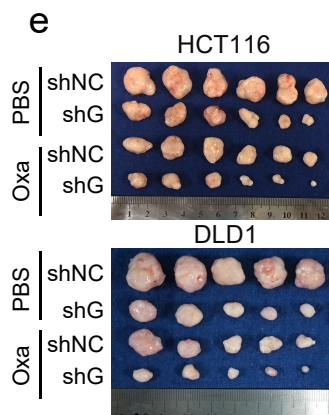
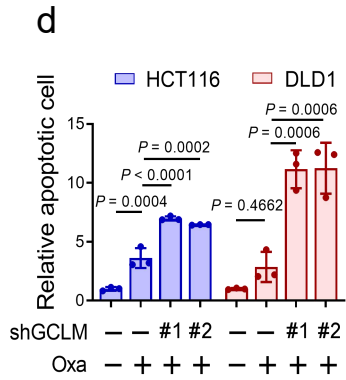
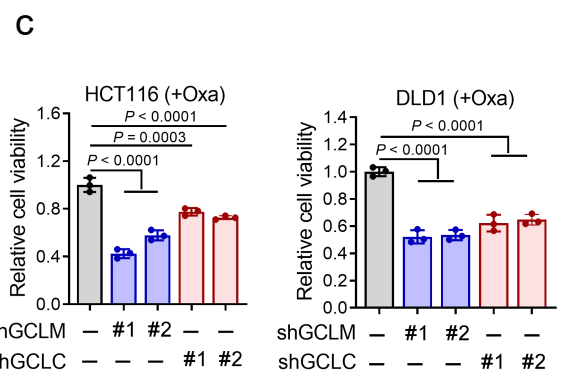
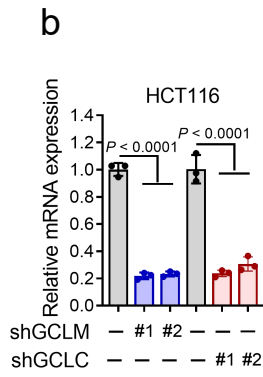
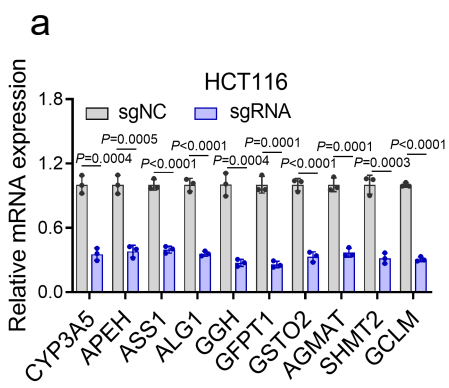
**Supplementary Figure 6:** Phosphorylation of GCLM at T17 contributes to CRC chemoresistance in vivo.

**Supplementary Figure 7:** Nuclear GCLM is highly expressed in tumours and indicates a poor prognosis.

**Supplementary Figure 8:** The gating strategy used for apoptosis assays in this study.

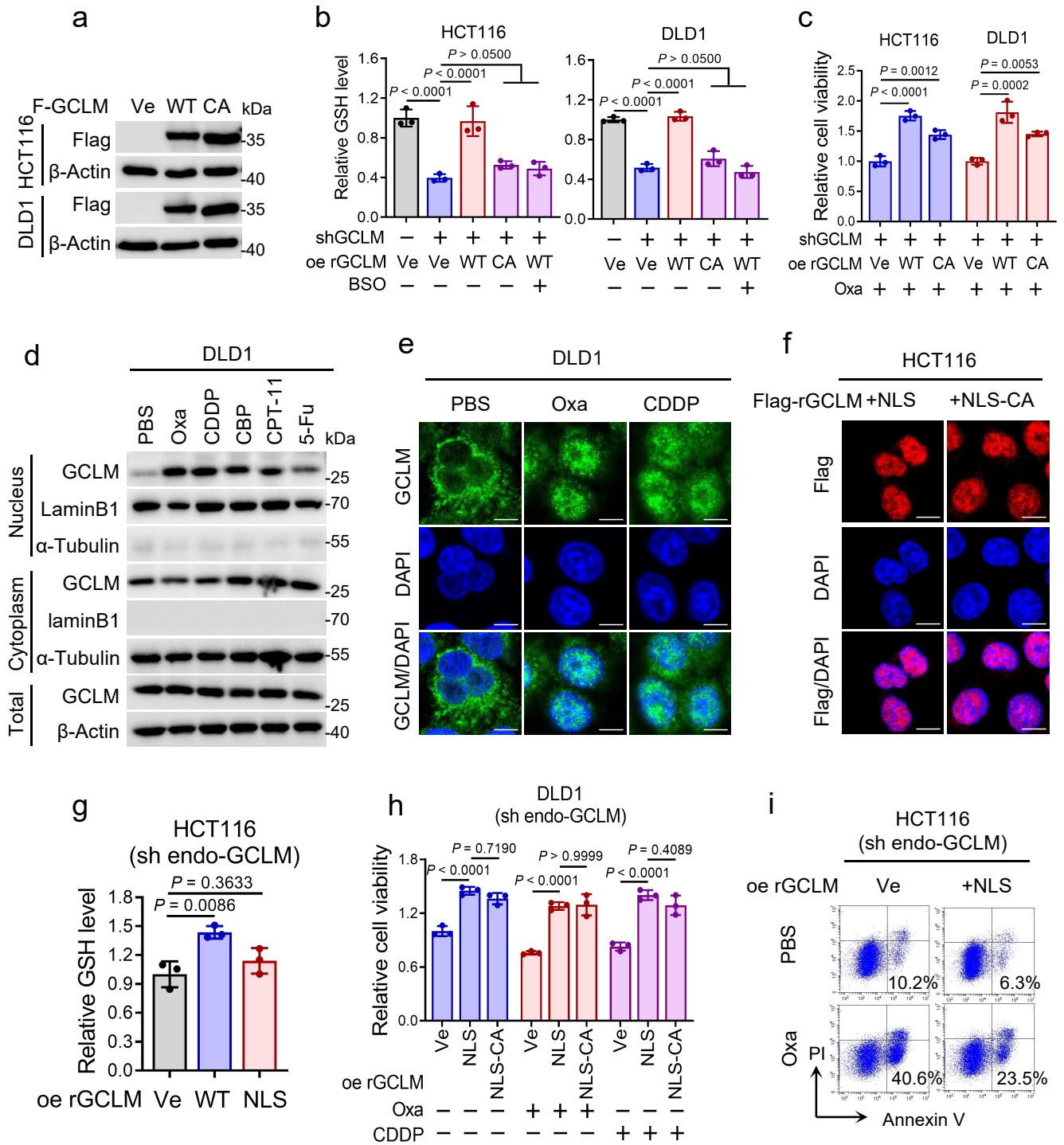
**Supplementary Table 1:** Correlation analysis for clinicopathologic variables in nuclear GCLM expression among 406 CRC patients.

**Supplementary Table 2:** Univariate and multivariate analysis of prognostic factors for overall survival among 406 CRC patients.



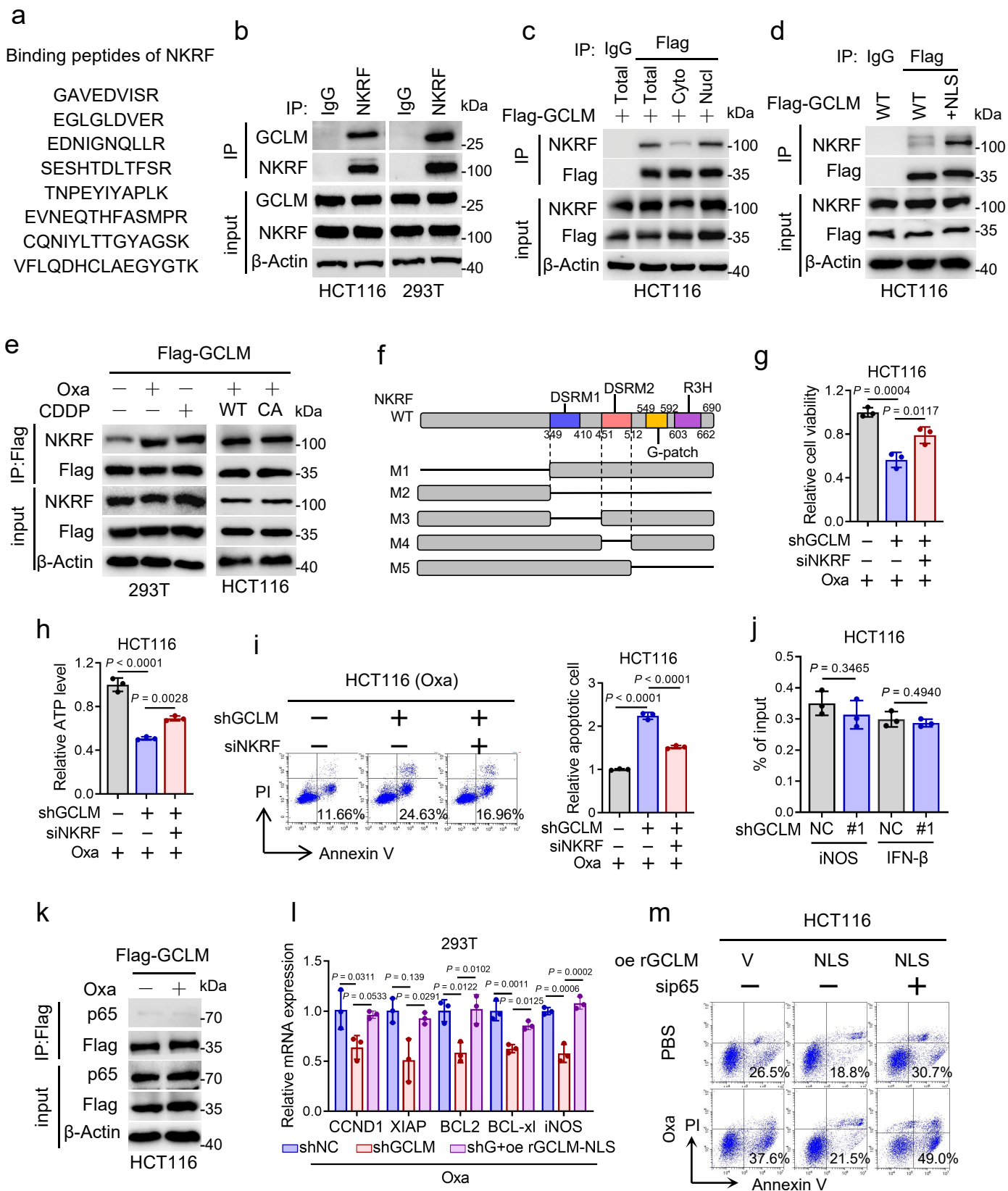
**Supplementary Fig. 1 GCLM depletion enhances the chemosensitivity of CRC cells to oxaliplatin.**

**a** Q-PCR analysis of the candidate gene expression after knocking out CYP3A5, APEH, ASS1, ALG1, GGH, GFPT1, GSTO2, AGMAT, SHMT2 or GCLM in HCT116 cells. **b** Q-PCR analysis of GCLM or GCLC expression after knocking down GCLM or GCLC in HCT116 cells. **c** Viability of HCT116 or DLD1 cells after knocking down GCLM or GCLC with oxaliplatin treatment (Oxa, 40  $\mu$ M for HCT116, 80  $\mu$ M for DLD1, 24 h). **d** Quantification analysis of the percentages of apoptotic cells in **Figure 1 e**. Photographs of the excised tumors from HCT116 and DLD1 cells based CDX models (HCT116, n = 6 per group; DLD1, n = 5 per group). **f** Statistical analysis of CDX tumor volume and weight in nude mice after implantation of GCLM-knockdown or control DLD1 cells ( $2 \times 10^6$ ), followed by intraperitoneal injections of PBS or oxaliplatin (5 mg/kg). **g** Illustration of the methodology used to establish CRC PDX models. **h** IHC staining showing GCLM in PDX-based paraffin-embedded subcutaneous tumor sections. Scale bar = 50  $\mu$ m. **i** Photographs of the excised tumors from PDX #1 (left) and PDX #2 (right) models (n = 6 per group). **j** H&E, IHC staining of Ki67, TUNEL assay and Masson's trichrome staining in PDX #2-based paraffin-embedded subcutaneous tumor sections. The red arrowheads indicate the positive cell of TUNEL staining. Scale bar = 50  $\mu$ m. **k** Quantification of the proliferation index (Ki67 staining) and apoptotic index (TUNEL assay) of the PDX #2 models. n = 3 biologically independent experiments in **a-d**, n = 5 mice in **f** and n = 6 mice in **k**. All the data are presented as the mean  $\pm$  S.D. The *P* values were calculated by two-tailed unpaired Student's *t* test (**a**), one-way ANOVA (**b**, **c**, **d**, **f** right and **k**), and two-way ANOVA (**f** left).



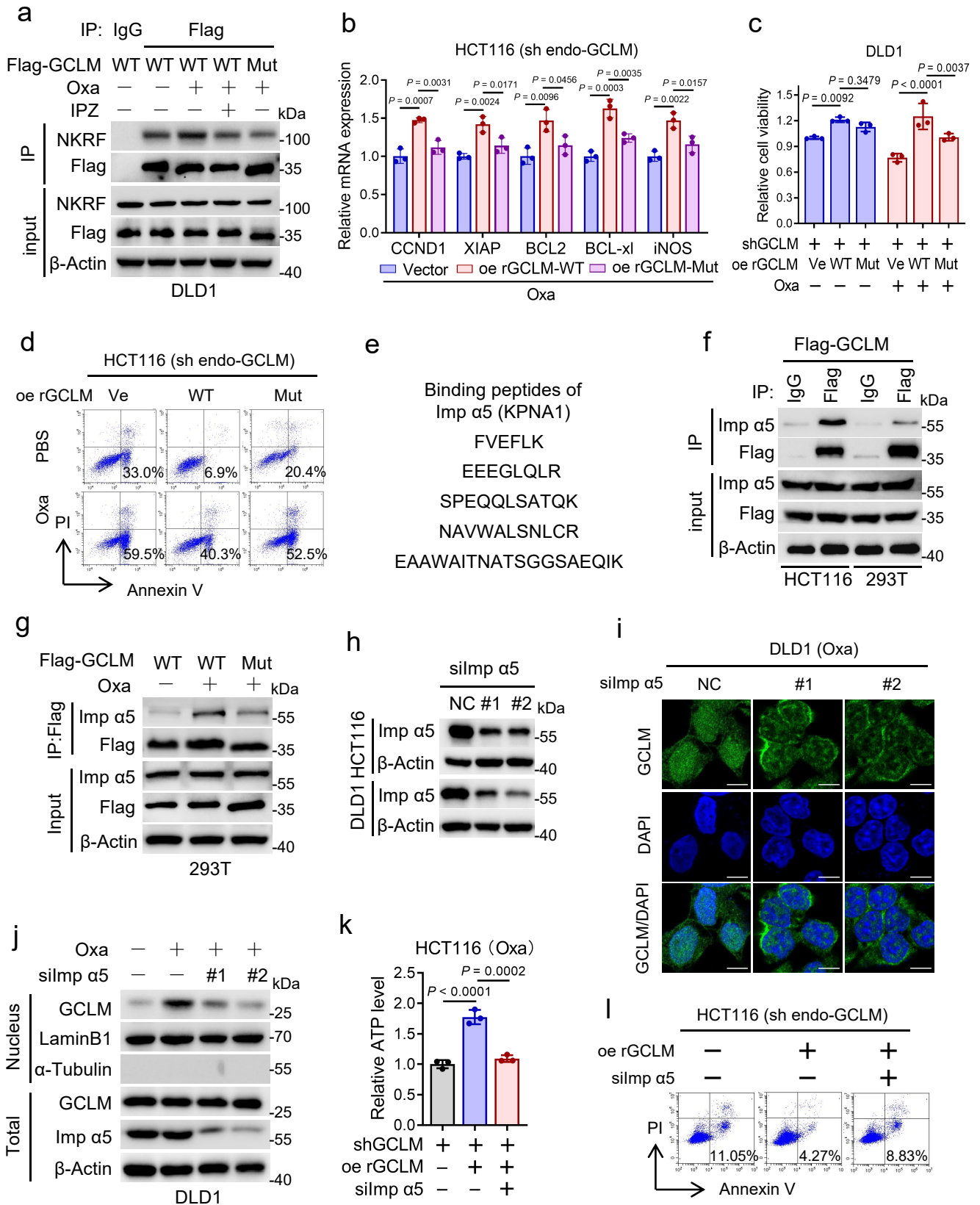
## **Supplementary Fig. 2 GCLM translocates to the nucleus up platinum drug treatment.**

**a** IB analysis of GCLM protein expression in HCT116 and DLD1 cells overexpressing control, rGCLM WT or C193/194A mutant (CA). **b** The GSH level analysis of endogenous GCLM-knockdown HCT116 and DLD1 cells overexpressing control, rGCLM WT or C193/194A mutant (CA) with or without the treatment of BSO (150  $\mu$ M, 24 h). **c** Cell viability of endogenous GCLM-knockdown HCT116 and DLD1 cells overexpressing control, rGCLM WT or C193/194A mutant in the presence of oxaliplatin (40  $\mu$ M for HCT116 and 80  $\mu$ M for DLD1, 24 h). **d** IB detection of total, cytoplasmic and nuclear GCLM expression in DLD1 cells treated with chemotherapeutic drugs including oxaliplatin (Oxa, 80  $\mu$ M), cisplatin (CDDP, 80  $\mu$ M), carboplatin (CBP, 80  $\mu$ M), irinotecan (CPT-11, 40  $\mu$ M) and 5-fluorouracil (5-FU, 40  $\mu$ M) for 24 h. **e** IF staining showing the localization of GCLM in DLD1 cells with the treatment of oxaliplatin or cisplatin (80  $\mu$ M, 24 h). Scale bar = 10  $\mu$ m. **f** IF staining images of the localization of GCLM in HCT116 cells overexpressing nuclear GCLM (+NLS) or C193/194A mutant (+NLS-CA). Scale bar = 10  $\mu$ m. **g** The GSH level analysis of GCLM knockdown HCT116 cells overexpressing control, rGCLM WT or nuclear GCLM (rGCLM NLS). **h** Cell viability of GCLM-knockdown DLD1 cells overexpressing control, nuclear GCLM WT (rGCLM NLS) or C193/194A mutant (CA) with PBS, oxaliplatin or cisplatin treatment (80  $\mu$ M, 24 h). **i** Annexin V/PI analysis the apoptotic cells in GCLM-knockdown HCT116 cells overexpressing control, nuclear GCLM (rGCLM NLS) with or without oxaliplatin treatment (40  $\mu$ M, 24 h). IB experiments were repeated three times and  $n = 3$  biologically independent experiments in **b**, **c**, **g**, **h**. All the data are presented as the mean  $\pm$  S.D. The  $P$  values were calculated by one-way ANOVA (**b**, **c**, **g**) and two-way ANOVA (**h**).



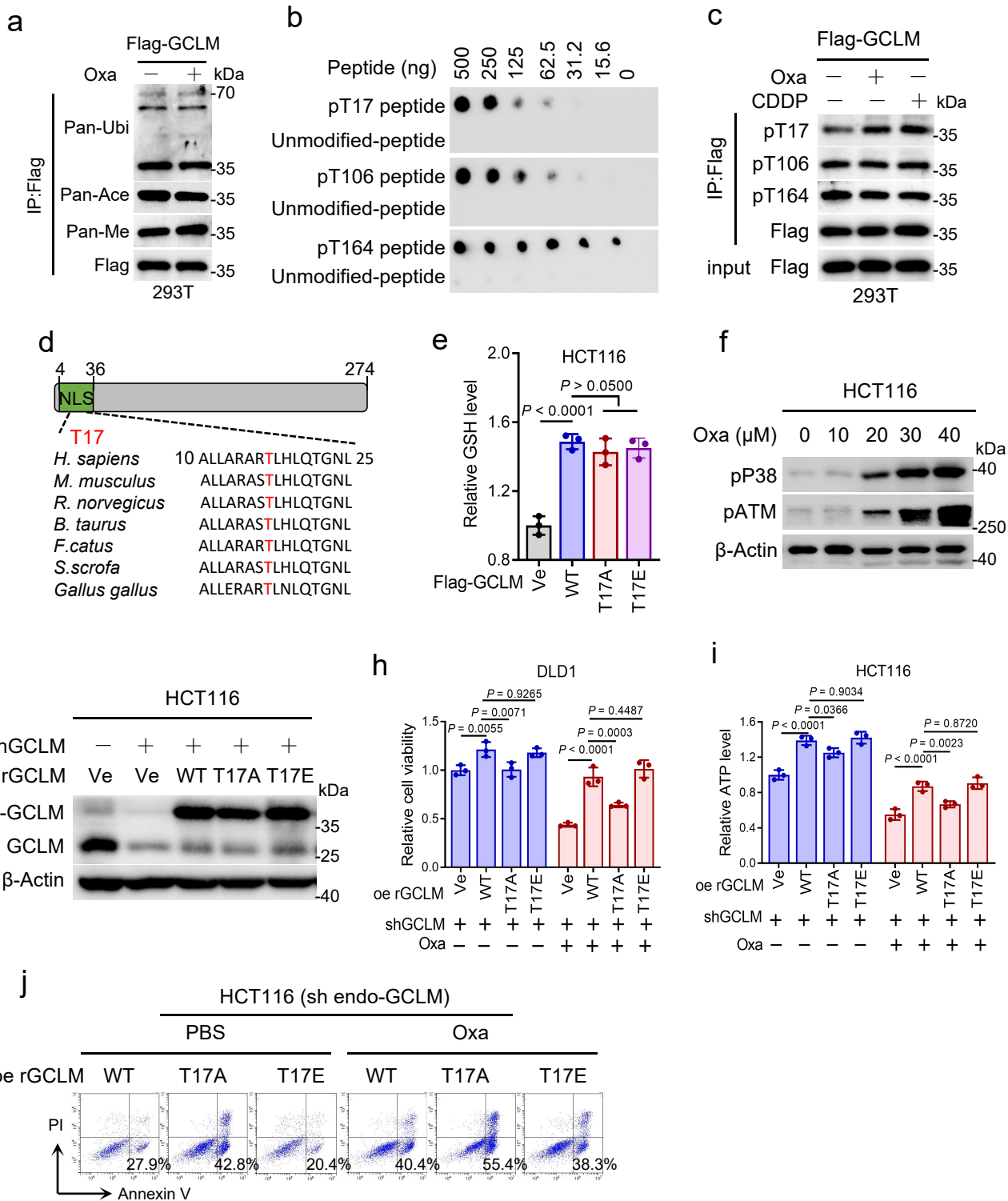
### **Supplementary Fig. 3 Nuclear GCLM interacts with NKRF to orchestrate NF- $\kappa$ B activity and chemoresistance.**

**a** The peptide sequences of NKRF bound by nuclear GCLM in 293T cells under oxaliplatin treatment (40  $\mu$ M, 24 h) through LC-MS/MS analysis in **Figure 3a**. **b** Co-IP analysis showing the level of GCLM bound by NKRF using anti-NKRF or IgG antibody. **c** Co-IP analysis demonstrating the level of NKRF bound by total, cytoplasmic and nuclear GCLM. **d** Co-IP analysis showing the interaction of GCLM and NKRF in HCT116 cells overexpressing Flag-tagged GCLM WT or nuclear GCLM (+NLS). **e** Co-IP analysis showing the interaction of GCLM and NKRF in 293T cells treated with oxaliplatin (Oxa) or cisplatin (CDDP) (40  $\mu$ M, 24 h) (left), and in HCT116 cells overexpressing Flag-tagged GCLM WT or C193/194A mutant treated with oxaliplatin (40  $\mu$ M, 24 h) (right). **f** Schematic illustration of NKRF protein containing four main domains. The strategy for mutating NKRF is also shown. **g-i** GCLM was depleted in HCT116 cells with or without importin  $\alpha$ 5 inhibition under oxaliplatin treatment (40  $\mu$ M, 24 h). cell viability (**g**), ATP level (**h**) and apoptotic cells (**i**) were detected. **j** Q-PCR analysis after ChIP analysis showing the occupancy of NKRF on the negative regulatory elements (NRE) of *iNOS* and *IFN- $\beta$*  promoter. **k** Co-IP analysis showing the interaction of GCLM and p65 in HCT116 cells with or without oxaliplatin treatment (40  $\mu$ M, 24 h). **l** Q-PCR analysis of the expression of NF- $\kappa$ B/p65-targeted genes (CCND1, XIAP, BCL2, BCL-xl, and iNOS) in 293T cells when depleting GCLM and re-expressing nuclear GCLM (+NLS) in the presence of oxaliplatin (40  $\mu$ M, 24 h). **m** Annexin V/PI analysis the apoptotic cells in nuclear GCLM-overexpressed HCT116 cells with control or p65 silencing with or without oxaliplatin treatment (40  $\mu$ M, 24 h). IB experiments were repeated three times and  $n = 3$  biologically independent experiments in **g-j, l**. All the data are presented as the mean  $\pm$  S.D. The  $P$  values were calculated by one-way ANOVA (**g-i, l**) and two-tailed unpaired Student's  $t$  test (**j**).



**Supplementary Fig. 4 Platinum drugs promote GCLM nuclear localization via GCLM binding to importin  $\alpha 5$ .**

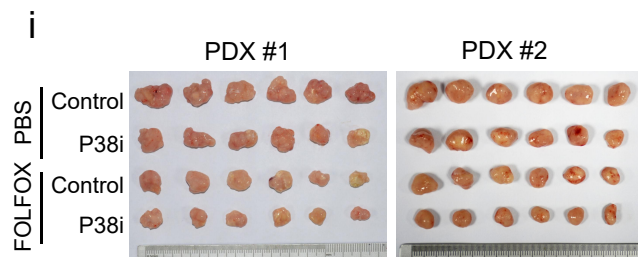
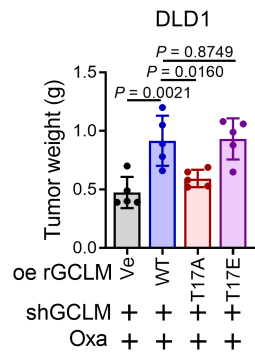
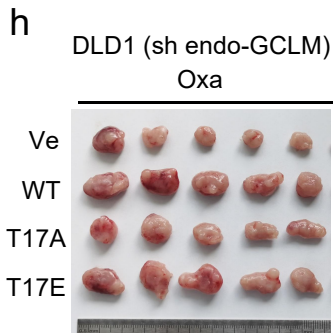
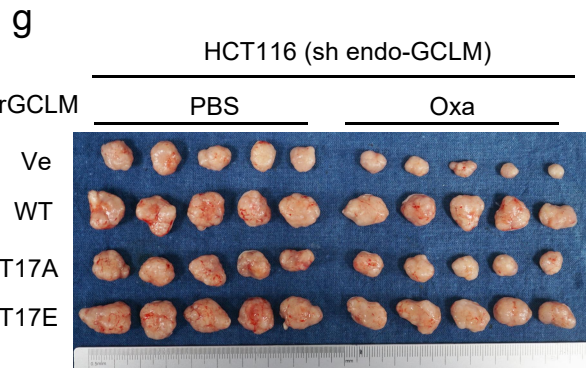
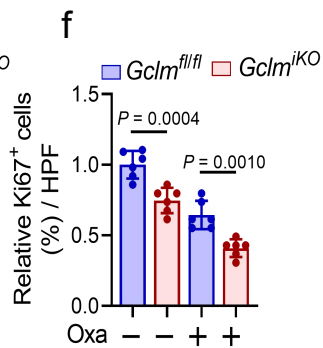
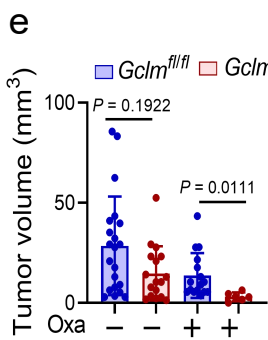
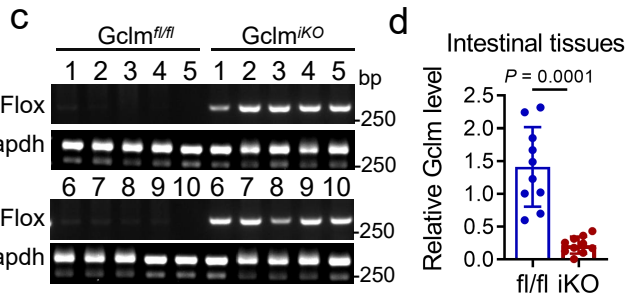
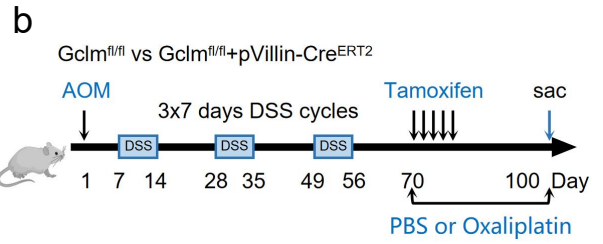
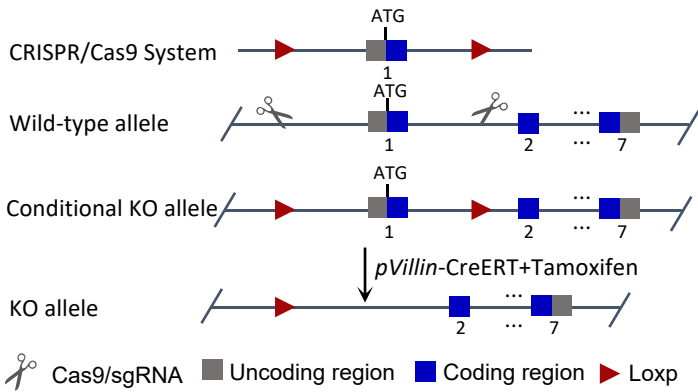
**a** DLD1 cells overexpressed Flag-tagged GCLM WT or GCLM-NLS Mut with oxaliplatin (80  $\mu$ M, 24 h) or IPZ treatment (40  $\mu$ M, 24 h). Co-IP analysis showing the interaction of GCLM and NKRF. **b, c, d** GCLM knockdown HCT116 or DLD1 cells overexpressed vector Flag-tagged GCLM WT or GCLM-NLS Mut with or without oxaliplatin treatment (40  $\mu$ M, 24 h). Q-PCR analysis of the expression of NF- $\kappa$ B/p65-targeted genes (CCND1, XIAP, BCL2, BCL-xl, and iNOS) (**b**), cell viability (**c**) and apoptotic cells analysis were performed. **e** The peptide sequences of importin  $\alpha 5$  bound by total GCLM in HCT116 cells through the LC-MS/MS analysis under oxaliplatin treatment (40  $\mu$ M, 24 h). **f** HCT116 or 293T cells overexpressed Flag-tagged GCLM WT under oxaliplatin treatment (40  $\mu$ M, 24 h). Co-IP analysis showing the interaction of importin  $\alpha 5$  and GCLM using anti-Flag or IgG antibody. **g** Co-IP analysis showing the GCLM-importin  $\alpha 5$  interaction in 293T cells overexpressing Flag-tagged GCLM WT or GCLM-NLS Mut with or without oxaliplatin treatment (40  $\mu$ M, 24 h). **h** IB analysis the level of importin  $\alpha 5$  in control or importin  $\alpha 5$  silenced HCT116 and DLD1 cells. **i, j** IF staining showed the localization of GCLM (**i**) and IB detected nuclear and total GCLM expression (**j**) in DLD1 cells with control or importin  $\alpha 5$  silencing in presence or absence of oxaliplatin treatment (80  $\mu$ M, 24 h). Scale bar = 10  $\mu$ m. **k, l** GCLM knockdown HCT116 cells overexpressed vector or rGCLM WT with control or importin  $\alpha 5$  silencing under oxaliplatin treatment (40  $\mu$ M, 24 h). ATP level (**k**) and apoptotic cells (**l**) were detected. IB experiments were repeated three times and  $n = 3$  biologically independent experiments in **b, c, k**. All the data are presented as the mean  $\pm$  S.D. The  $P$  values were calculated by one-way ANOVA (**b, k**) and two-way ANOVA (**c**).



**Supplementary Fig. 5 P38 MPAK-mediated phosphorylation of GCLM participates in platinum drug-induced nuclear localization of GCLM.**

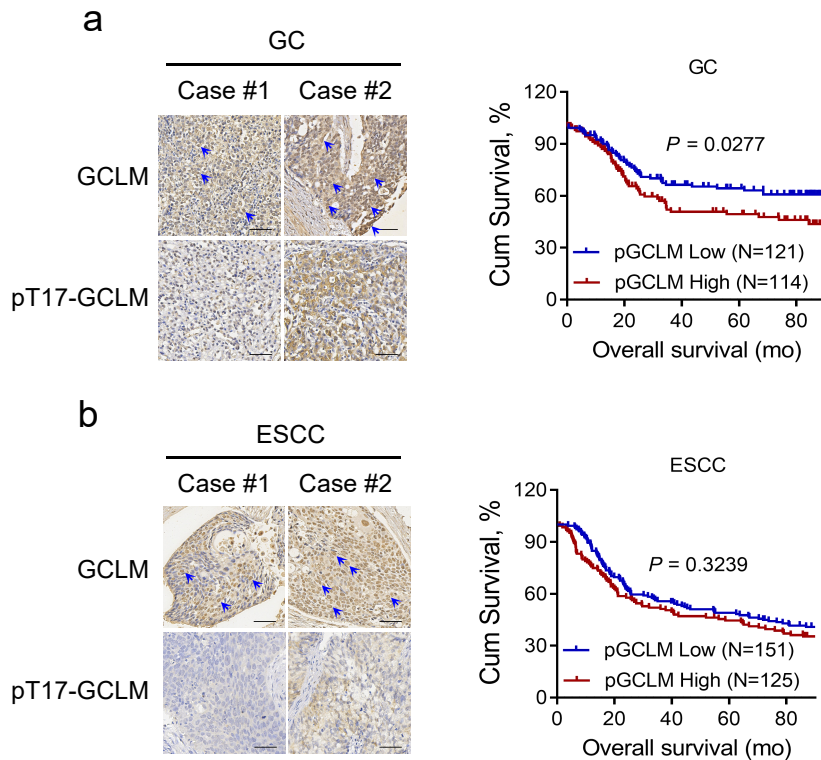
**a** IP analysis demonstrating the common post-translational modifications level of GCLM in 293T cells overexpressing Flag-tagged GCLM and treated with oxaliplatin (40  $\mu$ M, 24 h), including ubiquitination (Pan-Ubi), acetylation (Pan-Ace) and methylation (Pan-Me). **b** Dot blot analysis showing the specificity of anti-pThr17/Thr106/Thr164 antibodies treated with different concentrations of specific and unmodified peptides. **c** IP analysis showing the level of GCLM phosphorylated at Thr17, Thr106 and Thr164 in 293T cells overexpressing Flag-tagged GCLM and treated with or without oxaliplatin or cisplatin (40  $\mu$ M, 24 h). **d** Sequence alignment of phosphorylated peptides of GCLM at Thr17 among indicated species. **e** The GSH level analysis of HCT116 cells overexpressing Flag-tagged GCLM WT or T17A, T17E mutants. **f** IB detection of phosphorylated P38 MAPK (pP38) and ATM (pATM) level in HCT116 cells treated with different concentrations of oxaliplatin (24 h). **g** IB detection of GCLM level in control or GCLM knockdown HCT116 cells overexpressing rGCLM WT or T17A, T17E mutants. **h** Cell viability of GCLM knockdown DLD1 cells overexpressing rGCLM WT or T17A, T17E mutants with or without oxaliplatin treatment (80  $\mu$ M, 24 h). **i, j** ATP level (**i**) and apoptotic cells (**j**) analysis in GCLM knockdown HCT116 cells overexpressing rGCLM WT or T17A, T17E mutants with or without oxaliplatin treatment (40  $\mu$ M, 24 h). IB experiments were repeated three times and  $n = 3$  biologically independent experiments in **e, h, i**. All the data are presented as the mean  $\pm$  S.D. The  $P$  values were calculated by one-way ANOVA (**e**) and two-way ANOVA (**h, i**).

**a** Editing strategy for conditional intestinal knockout mouse *Gclm* gene



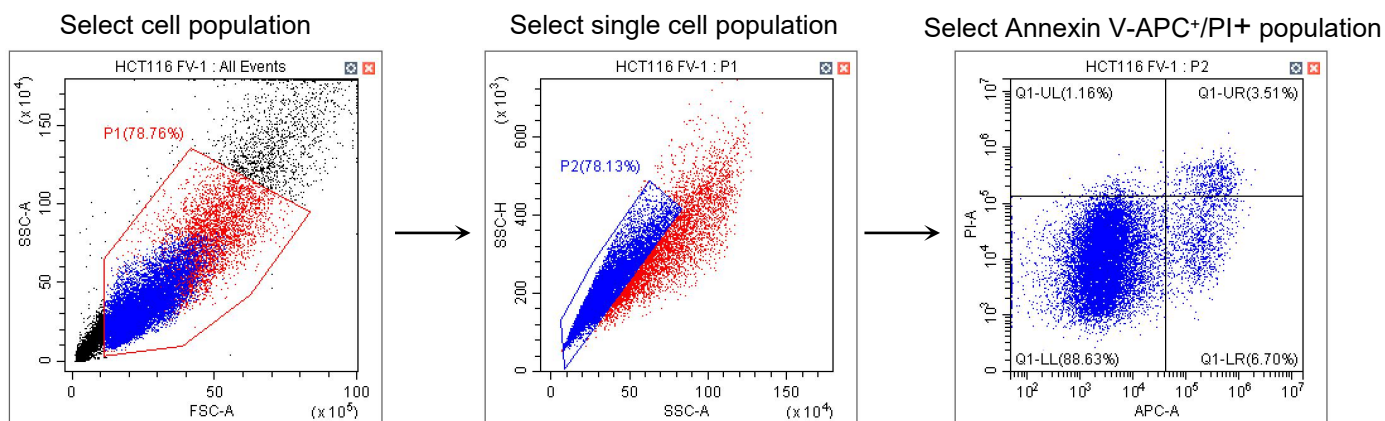
## Supplementary Fig. 6 Phosphorylation of GCLM at T17 contributes to CRC chemoresistance in vivo.

**a** Illustration of the editing strategy for conditional intestinal knockout mouse *Gclm* gene by expressing Cre recombinase under the control of the pVillin gene promoter (pVillin-CreERT2), an intestine-specific promoter. **b** Experimental design for the mouse model of AOM/DSS-induced spontaneous CRC established in *Gclm<sup>fl/fl</sup>* and *Gclm<sup>iKO</sup>* mice, followed by intraperitoneal injection of PBS or oxaliplatin (5 mg/kg). **c** Agarose gel electrophoresis analysis after PCR analysis of the DNA from mouse intestine tissue, which revealed a 377 bp band after the loxp sequence were cut in the KO allele not the wild-type or floxed allele whose products (7000bp) cannot be amplified. *Gapdh* was included as a loading control. **d** Q-PCR analysis showing the expression of *Gclm* in intestine of spontaneous tumors from *Gclm<sup>fl/fl</sup>* and *Gclm<sup>iKO</sup>* mice after tamoxifen (15 mg/kg for 5 days) treatment. **e, f** Statistical analysis of tumor size of each spontaneous tumor (**e**) and quantification for Ki67 staining (**f**) in *Gclm<sup>fl/fl</sup>* and *Gclm<sup>iKO</sup>* mice treated with PBS or oxaliplatin (5 mg/kg). **g, h** Photographs and weight of CDX tumor after the implantation of endogenous GCLM-knockdown HCT116 (**g**) and DLD1 (**h**) cells ( $2 \times 10^6$ ), which overexpressed rGCLM WT or T17A, T17E mutants, followed by intraperitoneal injections of PBS or oxaliplatin (5 mg/kg) ( $n = 5$  per group). **i** Photographs of PDX models followed by intraperitoneal injections of control or P38 inhibitor (P38i, SB203580, 5 mg/kg) and FOLFOX (oxaliplatin 5 mg/kg, 5-fluorouracil 25 mg/kg) ( $n = 6$  per group).  $n = 10$  mice in **d**,  $n = 6$  mice in **e, f** and  $n = 5$  mice in **h**. All the data are presented as mean  $\pm$  S.D. The *P* values were calculated by two-tailed unpaired Student's *t* test (**d**) and one-way ANOVA (**e, f, h** right).



**Supplementary Fig. 7 Nuclear GCLM is highly expressed in tumours and indicates a poor prognosis.**

**a, b** IHC staining for nuclear GCLM expression in (nGCLM, only focusing on GCLM staining in the nucleus, as shown by blue arrowheads) and the level of GCLM phosphorylated at Thr17 (pT17-GCLM) in GC (n = 235, GC tissue specimens) or ESCC (n = 276, ESCC tissue specimens) tissues. GC, gastric carcinoma, ESCC, esophageal squamous cell carcinoma. Scale bar = 50  $\mu$ m (**a, b** left). Overall survival assays of patients with GC or ESCC based on pT17-GCLM expression. We categorized proteins level as low or high compared with the median value of IHC score (**a, b** right). The *P* values were calculated by Kaplan-Meier analysis (log-rank test) (**a, b** right).



**Supplementary Fig. 8 The gating strategy used for apoptosis assays in this study.**

Apoptosis was analyzed with a Annexin V/PI Kit and conducted with a flow cytometer using APC (638nm) and PI (488nm) channel.

Supplementary Table 1: Correlation analysis for clinicopathologic variables in nuclear GCLM expression among 406 CRC patients

Variable	Low nGCLM n (%)	High nGCLM n (%)	<i>P</i> value
Total	183 (45.1)	223 (54.9)	
Age, years			0.690
≤ 57	99 (54.1)	116 (52.0)	
> 57	84 (45.9)	107(48.0)	
Sex			1.000
Male	110 (60.1)	133 (59.6)	
Female	73 (39.9)	90 (40.4)	
Clinical stage			<0.001
I - II	81 (44.3)	49 (22.0)	
III-IV	102 (55.7)	174 (78.0)	
Histological grade			0.230
Well/moderate	148 (80.9)	169 (75.8)	
Poor and others	35 (19.1)	54 (24.2)	
Tumor depth			0.166
m/sm/mp	21 (11.5)	16 (7.2)	
ss/se/si	162 (88.5)	207 (92.8)	
Vascular invasion			0.416
Absent	127(88.2)	148(84.6)	
Present	17 (11.8)	27 (15.4)	
Perineural invasion			0.647
Absent	84 (58.3)	107 (61.1)	
Present	60(41.7)	68 (38.9)	

The *P* values were determined by two-sided Chi-square test. Abbreviations: m: tumor invasion of mucosa; sm: submucosa; mp: muscularis propria; ss:subserosa; se: serosa penetration; si: invasion to adjacent structures.

Supplementary Table 2: Univariate and multivariate analysis of prognostic factors for overall survival among 406 CRC patients

Factors	Univariate		Multivariate*	
	HR (95% CI)	<i>P</i> value	HR (95% CI)	<i>P</i> value
Age (≤57/>57)	1.153 (0.750-1.772)	0.516	/	/
Sex (male/female)	1.863(1.177-2.947)	0.008	/	/
TNM stage ( I - II /III-IV)	3.480 (1.998-6.063)	<0.001	/	/
Histological grade (Well,moderate/ Poor and others)	1.743(1.062-2.861)	0.028	1.972 (1.046-3.716)	0.036
Tumor depth (m, sm, mp/ss, se, si)	1.820 (0.776-4.269)	0.168	/	/
Vascular invasion (absent/present)	2.088 (1.015-4.293)	0.045	/	/
Perineural invasion (absent/present)	2.204 (1.243-3.908)	0.007	1.870 (1.021-3.472)	0.043
nGCLM expression (low/high)	1.701 (1.093-2.648)	0.019	2.334 (1.241-4.389)	0.009

The *P* value was determined by the univariate and multivariate cox regression analysis. All the statistical tests were two-sided. Abbreviations: CRC: Colorectal cancer; m: tumor invasion of mucosa; sm: submucosa; mp: muscularis propria; ss:subserosa; se: serosa penetration; si: invasion to adjacent structures. HR: hazard ratio; CI: confidence interval.

\* For the multivariate model, HR and *P* values were shown by backward method only.